PHYSICAL REVIEW E **77**, 030601(R) (2008)

Observation of a liquid-to-layered transition in thin liquid films when surface and interface regions overlap

Dong Ryeol Lee,[1] Pulak Dutta,[2,*] and Chung-Jong Yu[3,†]

[1]*Pohang Accelerator Laboratory and Department of Physics, Pohang University of Science and Technology, Pohang 790-784, Korea*

[2]*Department of Physics and Astronomy, Northwestern University, Evanston, Illinois 60208-3112, USA*

[3]*Pohang Accelerator Laboratory, Pohang 790-784, Korea*

(Received 30 August 2007; revised manuscript received 14 November 2007; published 14 March 2008)

We have used x-ray reflectivity to study the coupling of surface and interface layering in a molecularly thin normal liquid [tetrakis(2-ethylhexoxy)silane (TEHOS)], as a function of temperature and film thickness. The best fits to the data were obtained with an electron density model that consists of a uniform density component superimposed upon molecular-scale density oscillations (layers). The two types of layer profiles were observed to vary with temperature from 187–286 K. The amount of material in the molecular layers increases as that in the uniform density layer decreases, with the onset of liquid-to-layered transition occurring at a total film thickness of ~40 Å (about twice the bulk correlation length of TEHOS).

DOI: 10.1103/PhysRevE.77.030601   PACS number(s): 68.15.+e, 68.03.Hj, 68.08.De

Thin liquid films are common in a wide variety of applications such as lubrication, spreading, wetting, adhesion, melting, and nucleation, and are thus relevant to many chemical, biological, geophysical, and industrial processes. It is known that the properties of thin liquid films cannot simply be deduced from those of corresponding bulk liquids. Many attempts have been made to probe their structures to understand their properties [1–18]. Both metallic and nonmetallic liquids have been observed to show molecular layering near and parallel to a hard wall, as long as the wall is smooth compared to the molecule size [1–6]. Metallic liquids show layering at the free surface as well [7–10]. In contrast, molecular layering at the free surface had not been reported for nonmetallic liquids, except for solid monolayer formation just above the bulk melting point in alkanes [11]. It has been suggested that the difference between metallic and nonmetallic liquids at the free surface originates from the free surface width, which is so large for nonmetallic liquids as to suppress the layering [17]. Chacón *et al.* [18], however, showed in Monte Carlo simulations that the difference is whether a liquid can reach a temperature $T \approx 0.2T_c$ without freezing. Shpyrko *et al.* [12] studied liquid potassium and water, which have a similar free surface width, but potassium showed layering while water did not. Mo *et al.* [13] directly observed free surface layering in a nonmetallic liquid, tetrakis(2-ethylhexoxy)silane (TEHOS), at $T \approx 0.23T_c$. TEHOS molecules are spherical with size ~10 Å, nonpolar, nonreactive, nonliquid crystalline, and nonentangling. It remains liquid down to 190 K [13]. The fact that TEHOS shows surface layering motivated us to study molecularly thin TEHOS films in the "cold phase" where there is both interfacial layering and free surface layering.

Silicon substrates ($3 \times 1 \times 0.07$ cm^3) were carved along the cleaving facet with a diamond scriber to a size of 1×1 cm^2. They were cleaned in a strong oxidizer, 30:70 vol % hydrogen peroxide (30%):sulfuric acid for 30 minutes at ~90 °C, rinsed with ample amount of pure water (>18.0 Ω cm), and left in water until use. TEHOS (>95% pure, Gelest) solution was prepared by dissolving 60–150 μl TEHOS in 25 cc of hexane (98.5% pure, Sigma-Aldrich). To prepare a thin TEHOS film, a silicon piece was blown dry with 99% nitrogen gas, dipped in the TEHOS solution, and withdrawn at a speed of ~1 cm/sec. The solvent evaporates, leaving an ultrathin film of TEHOS. Hexane has an electron density about 0.65 times that of TEHOS, which we do not see, and thus none of the layers reported here can be attributed to hexane. We then cleaved the silicon substrate carefully while not touching the substrate surface and attached it to the sample holder using carbon tape. The sample holder was put into a plastic bag and capped with a vacuum-tight Be dome under helium flow. The sample holder with the Be dome was mounted in a displex system. A liquid film ~5000 Å thick was also prepared as described in Ref. [3] to obtain reference data. X-ray reflectivity measurements were done with a Huber kappa diffractometer and performed at the 5A HFXS wiggler beamline of Pohang Accelerator Laboratory. The x-ray energy was 11.6 keV and the beam size was measured to be 0.3×1.0 mm^2 at the sample position.

Figure 1 shows a typical behavior of the normalized reflectivity data vs temperature for films of thicknesses from 55–200 Å at 286 K on a smooth silicon surface with native oxide. The apparent thickness was obtained using the uniform density model with the error-function-broadened interfaces fit to the reflectivity data [2]. The TEHOS film at 286 K shows Kiessig fringes indicating a thickness of ~61 Å with a broad "hump" centered at $q_z \sim 0.65$ Å^{-1} (where $q_z = 4\pi/\lambda \sin\theta$, λ is the wavelength of the incident x ray, and θ is the incident angle with respect to the sample surface). The hump is caused by internal layering near the solid-liquid interface [2]. It does not vary over the temperature range we studied, which is expected because the interfacial layering is solely due to the smooth hard wall effect [19]. We also obtained the same result for a ~5000 Å thick film (not shown here). The apparent film thickness changes as the temperature changes. The data will be shown later.

At lower temperatures, fringes appear in the high q_z re-

*pdutta@northwestern.edu

†cjyu@postech.ac.kr

    ©2008 The American Physical Society

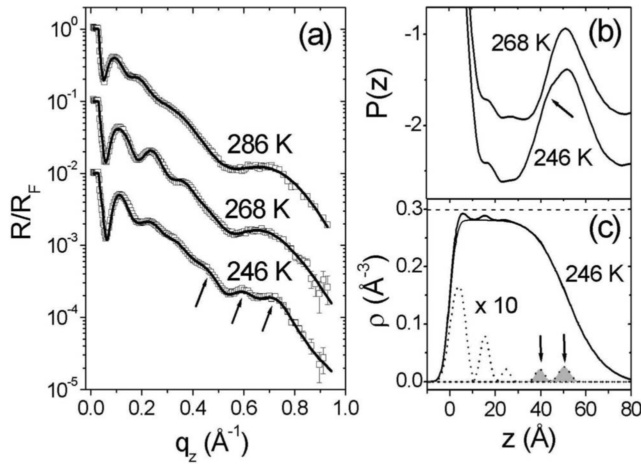

FIG. 1. (a) Normalized x-ray reflectivity data at different temperatures after background subtraction for a TEHOS film 61 Å thick at 286 K. The data are shifted vertically for clarity. The arrows indicate additional fringes developed at 246 K and below. Solid lines are the best fits using an electron density model consisting of the minimum necessary number of Gaussians and a uniform density layer for the liquid film with error-function broadened interfaces. (b) The Patterson functions, $P(z)$, in arbitrary units at selected temperatures as a function of the distance, z. The arrow at 246 K indicates the surface layering. (c) Thick solid line, the electron density profile for the data at 246 K after subtraction of the substrate part as a function of the distance, z, from the substrate surface; thin solid line, uniform electron density part; dashed line, Gaussians multiplied by 10 for a clear view. The shaded area with arrows measures the surface layering. The electron density of bulk TEHOS is shown as a dashed horizontal line at 0.3 Å^{-2}.

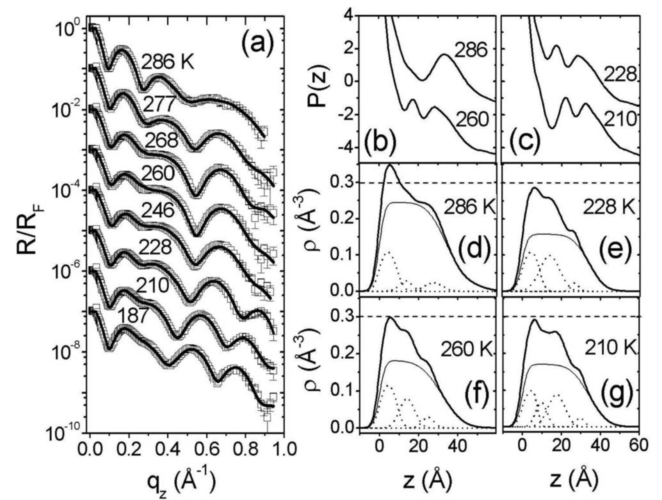

FIG. 2. (a) Normalized x-ray reflectivity data after background subtraction for a 33 Å thick TEHOS film at different temperatures. The data are shifted vertically for clarity. (b),(c) The Patterson functions at selected temperatures. Solid lines in (a) and the lines in (d)–(g) are described in the caption of Fig. 1.

gion, shown by arrows. This means that a density variation has developed near the interface or the surface, judging from the dip-to-dip distance of the fringes in q. However, the corresponding Patterson function shows that it occurs at the surface. The Patterson function is the Fourier transform of normalized reflectivity data and shows peaks whose positions correspond to the distances between regions where the density is changing rapidly. If there is a region with a very sharp density change, all the peak positions represent distances from that region [3]. Such a region in the TEHOS film is the interface, and this can be unambiguously determined using the uniform density model. Figure 1(b) shows two Patterson functions corresponding to the reflectivity data at 268 K and 246 K. Both of them are similar except the peak marked with an arrow evidently corresponding to the fringes seen in the higher q_z region in Fig. 1(a). The position of the peak shows that a density variation has developed near the surface.

To visualize the density variation, the electron density profiles were obtained using the Parratt algorithm [20] with many density slabs of equal width [21]. The model-independent results were further refined with the density model described in the caption of Fig. 1. Figure 1(c) displays the TEHOS electron density profile at 246 K, after subtracting the substrate density from the total electron density profiles. It shows three Gaussian layers separated by ~10 Å near the interface as expected [2]. The three additional fringes in the high q_z region at 246 K in Fig. 1(a) can be fitted with two additional Gaussians, shown shaded in Fig. 1(c). They are separated by ~10 Å, just like the interfacial layers, and indicate the development of molecular layering at the surface [13]. The temperature at which the surface layering starts to appear is ~246 K. The reflectivity data did not change much with temperature down to 187 K.

Figure 2 shows the reflectivity data, the corresponding Patterson functions at selected temperatures, and resulting electron density profiles for a ~33 Å thick film. This film does not show the fringes in the high q_z due to the surface layering at low temperatures as shown in Fig. 1(a), because these are superposed upon one of the Kiessig fringes located at 0.25–0.4 Å^{-1} and the hump resulting from the interfacial layering. This film is too thin to distinguish the surface layering from the interfacial layering. The reflectivity data in Fig. 2(a) do not change much from 277 K to 246 K, but significant changes occur below 246 K while the position of the first minimum around q_z=0.1 Å^{-1}, representing the apparent film thickness, stays unchanged. The Patterson functions in Figs. 2(b) and 2(c) show the change of internal structures with temperatures. At 286 K, the peak centered at ~33 Å in the Patterson function represents the film thickness. At 260 K and below, there are two peaks at ~20 Å and ~30 Å. In electron density profiles, the two peaks mean two density drops as one approaches the film surface. This can be seen in the fitted electron density profiles [Figs. 2(e)–2(g)]. It is also noted that the Gaussian layer centered at ~15 Å at 228 K separates into two at 210 K, although the apparent total thickness does not change much during the process. This is probably correlated with the overlap of surface and interface layering in this thinner film.

Figure 3(a) displays the reflectivity data for a ~53 Å thick film, and Fig. 3(c) displays the fitted electron density. The surface layering fringes show up in the high q_z region at 260 K and possibly 268 K as depicted by arrows, but they are merged with other fringes as temperature decreases. The

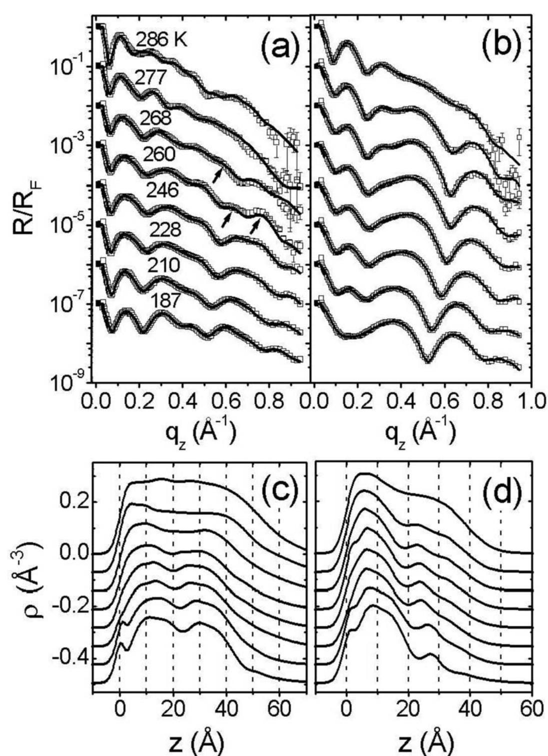

FIG. 3. Normalized x-ray reflectivity data for (a) 53 Å and (b) 38 Å thick films at different temperatures. Solid lines in (a) and (b) are described in the caption of Fig. 1(a). The electron density profiles corresponding to (a) and (b) are given in (c) and (d), respectively. Their temperatures are the same as those in (a) from top to bottom.

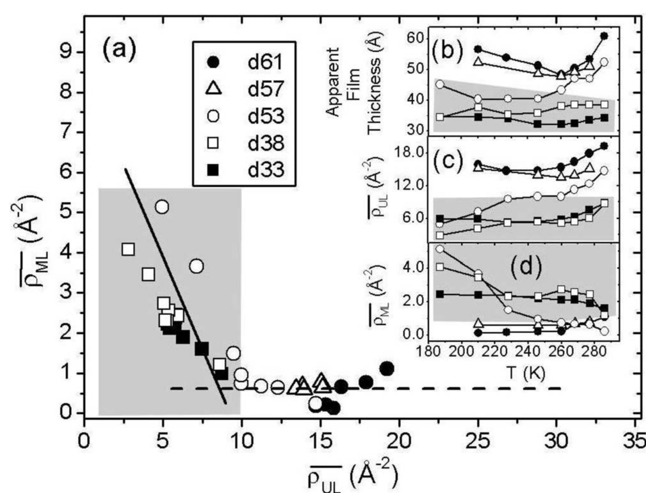

FIG. 4. (a) Summary curve showing the universal trend in integrated density of the layered component ($\overline{\rho_{\mathrm{ML}}}$) vs the integrated density of the uniform component ($\overline{\rho_{\mathrm{UL}}}$), obtained from the temperature-dependent data for five samples. The notation d# means for the film # Å thick. Insets show the apparent film thicknesses (b), $\overline{\rho_{\mathrm{UL}}}$ (c), and $\overline{\rho_{\mathrm{ML}}}$ (d) as functions of temperature. The shaded region for $\overline{\rho_{\mathrm{UL}}} < 10$ Å^{-2} in (a) indicates the liquid-to-layered transition region, and the corresponding regions in (b)–(d) are also shown shaded. The solid line and the dashed line are guides to the eye (see text for details).

fit results in Fig. 3(c) show quite different behaviors from that in Figs. 2(d)–2(g). There is a dip developed in the middle of the liquid density profile while two Gaussians separated by ~10 Å reside in each side of the dip. Figure 3(b) shows the reflectivity data for a film of thickness ~38 Å. The corresponding electron density profiles in Fig. 3(d) show a dip around 20 Å away from the interface. This dip separates an interface region and a surface region. Another observation is that both Figs. 2(e)–2(g) and 3(d) show slowly decreasing electron density profiles near the free surface. This type of density profile looks similar to the local pair correlation function at the free surface of a Lennard-Jones liquid [17].

The initial states of two films in Fig. 3 at 286 K show much weaker diffraction humps compared to that of the 33 Å thick film in Fig. 2. It is known that the amplitudes of the diffraction features are very sensitive to surface roughness [2], shear [22], impurities [23], etc. Thus different initial conditions in different samples may be responsible for the observed variations. Moreover, surface force measurements [19] show force oscillations as a function of liquid film thickness, and this implies that the degree of layer order also varies with thickness. Figures 3(c) and 3(d) show a narrow layer at the interface, which becomes clearer as temperature decreases. A similar unidentified narrow layer was also reported in a self-assembled monolayer (SAM) study at the solid-SAM interface [24]. These density profile variations do not affect the conclusions presented in this paper.

All our results indicate that the interfacial layering is modified when the apparent thickness is molecularly thin and the temperature is low enough that there is surface layering. The internal structure of the films continuously changes as temperature decreases, as is clear from the data in Figs. 2 and 3. It is also evident that the Gaussian layers can be thought of as molecular layers because they are usually separated by the molecule size. Fitting data for a number of samples are shown in Figs. 4(b)–4(d) as functions of temperature. In Fig. 4(b) we show the apparent film thickness; in Fig. 4(c) we show the integrated values of the uniform density layers ($\overline{\rho_{\mathrm{UL}}}$) within the liquid film; in Fig. 4(d) we show the integrated values of the molecular layers ($\overline{\rho_{\mathrm{ML}}}$). The temperature trends in Figs. 4(c) and 4(d) are not particularly clear because of the scatter in the data; however, a clear picture emerges when we compare $\overline{\rho_{\mathrm{ML}}}$ and $\overline{\rho_{\mathrm{UL}}}$ as shown in Fig. 4(a). Interfacial layering is not dependent upon temperature for 55–200 Å and 5000 Å thick films. This trend corresponds to the horizontal dashed line in Fig. 4(a). But below $\overline{\rho_{\mathrm{UL}}} = 10$ Å^{-2}, $\overline{\rho_{\mathrm{ML}}}$ begins to increase. The corresponding region in each of Figs. 4(a)–4(d) is shaded. The slope of the data points for $\overline{\rho_{\mathrm{UL}}} < 10$ Å^{-2} follows closely the solid line, which is the predicted dependence if a reduction in $\overline{\rho_{\mathrm{UL}}}$ corresponds to loss of molecules from the uniform density layer which are then all added to the molecular layer (i.e., the number of molecules is conserved). The shaded region in Fig. 4 is the liquid-to-layered transition region for an ultrathin film of TEHOS. As liquid films become thinner, our results imply that they will behave increasingly similar to an ordered phase. The shaded region in Fig. 4(b) shows that the

onset film thickness of the transition occurs at ~40 Å or twice the bulk correlation length of TEHOS [23].

One of the long-standing issues in nanoconfined liquids is what happens as a liquid film becomes thin (when two interfacial layers meet). A simple addition of each interfacial property cannot explain many nonlinear phenomena [19,25–30]. Structural probes such as x-ray scattering, however, have been unable to obtain very detailed data because of the difficulty of penetrating to and detecting the scattering from a small amount of liquid enclosed between solid substrates [31]. We have studied the overlap of interfacial layering and surface layering, while surface force apparatus studies probe the overlap of layering at two interfaces. These are not identical geometries, but it is reasonable to expect that similar trends will occur. Indeed, we have now confirmed through x-ray measurements that thinner films are better ordered, just as the force measurements have suggested.

We thank S. H. Choi and H. H. Lee for their help. This work was supported by the Korea Research Foundation Grant funded by the Korean Government (MOEHRD, Basic Research Promotion Fund) (KRF-2006-515-100942). One of us (P.D.) was supported by the U.S. National Science Foundation under Grant No. DMR-0705137.

[1] W. J. Huisman *et al.*, Nature (London) **390**, 379 (1997).
[2] C.-J. Yu, A. G. Richter, A. Datta, M. K. Durbin, and P. Dutta, Phys. Rev. Lett. **82**, 2326 (1999).
[3] C.-J. Yu *et al.*, Phys. Rev. E **63**, 021205 (2001).
[4] A. K. Doerr *et al.*, Europhys. Lett. **52**, 330 (2000).
[5] L. Cheng, P. Fenter, K. L. Nagy, M. L. Schlegel, and N. C. Sturchio, Phys. Rev. Lett. **87**, 156103 (2001).
[6] S. E. Donnelly *et al.*, Science **296**, 507 (2002).
[7] M. J. Regan *et al.*, Phys. Rev. Lett. **75**, 2498 (1995).
[8] M. J. Regan *et al.*, Phys. Rev. B **54**, 9730 (1996).
[9] E. DiMasi, H. Tostmann, B. M. Ocko, P. S. Pershan, and M. Deutsch, Phys. Rev. B **58**, R13419 (1998).
[10] H. Tostmann *et al.*, Phys. Rev. B **59**, 783 (1999).
[11] B. M. Ocko *et al.*, Phys. Rev. E **55**, 3164 (1997).
[12] O. Shpyrko *et al.*, Phys. Rev. B **69**, 245423 (2004).
[13] H. Mo *et al.*, Phys. Rev. Lett. **96**, 096107 (2006).
[14] M. Tolan, *X-ray Scattering from Soft-Matter Thin Films*, Springer Tracts in Modern Physics Vol. 148 (Springer, Berlin, 1999).
[15] M. Li, A. M. Tikhonov, D. J. Chaiko, and M. L. Schlossman, Phys. Rev. Lett. **86**, 5934 (2001).
[16] M. Li and M. L. Schlossman, Phys. Rev. E **65**, 061608 (2002).
[17] J. M. Soler, G. Fabricius, and E. Artacho, Surf. Sci. **482**, 1314 (2001).
[18] E. Chacón, M. Reinaldo-Falagan, E. Velasco, and P. Tarazona, Phys. Rev. Lett. **87**, 166101 (2001).
[19] J. N. Israelachvili, *Intermolecular and Surface Forces* (Academic, London, 1991).
[20] L. G. Parratt, Phys. Rev. **95**, 359 (1954).
[21] M. K. Sanyal *et al.*, Europhys. Lett. **36**, 265 (1996).
[22] C.-J. Yu *et al.*, Langmuir **19**, 9558 (2003).
[23] C.-J. Yu *et al.*, Europhys. Lett. **50**, 487 (2000).
[24] I. M. Tidswell *et al.*, Phys. Rev. B **41**, 1111 (1990).
[25] J. Klein and E. Kumacheva, Science **269**, 816 (1995).
[26] S. Granick, Phys. Today **52**, 26 (1999).
[27] S. Granick, Science **253**, 1374 (1991).
[28] H. K. Christenson, J. Phys.: Condens. Matter **13**, R95 (2001).
[29] S. T. Cui, P. T. Cummings, and H. D. Cochran, J. Chem. Phys. **114**, 7189 (2001).
[30] M. Urbakh *et al.*, Nature (London) **430**, 525 (2004).
[31] O. H. Seeck *et al.*, Europhys. Lett. **60**, 376 (2002).